

ELASTIC AND LENGTH–FORCE CHARACTERISTICS OF THE GASTROCNEMIUS OF THE HOPPING MOUSE (*NOTOMYS ALEXIS*) AND THE RAT (*RATTUS NORVEGICUS*)

G. J. C. ETTEMA

Department of Anatomical Sciences, The University of Queensland, Queensland 4072, Australia

Accepted 19 February 1996

Summary

The aim of this study was to compare the contractile and series elastic properties of terrestrial mammals that use bipedal *versus* quadrupedal gaits. The gastrocnemius muscle of the hopping mouse (body mass 30.2 ± 2.4 g, mean \pm S.D.) and the rat (313 ± 10.7 g) were compared with data from the literature for the wallaby and the kangaroo rat to distinguish scaling effects and locomotion-related effects on muscle properties. Contractile length–force properties and series elastic stiffness were measured *in situ* during maximal tetanic contractions.

The rat had a larger muscle-fibre-to-tendon-length ratio. The rat and hopping mouse showed similar normalised length–force characteristics of the gastrocnemius. Normalised stiffness in the hopping mouse was higher. The hopping mouse showed a higher capacity to store elastic energy per unit of contractile work capacity, as well as per unit of body mass.

Accounting for body size differences, the rat had a smaller relative muscle mass and thus smaller work capacity than the three hopping animals considered. This is in agreement with a quadrupedal *versus* bipedal locomotion style.

The differences in contractile and elastic properties of the gastrocnemius of the rat and hopping mouse seem to be closely related to locomotion patterns. Small animals seem to be able to utilise the storage and release of elastic energy to a far lesser extent than larger animals. However, even in animals as small as hopping mice, the storage and utilisation of elastic energy during locomotion is of functional significance and probably depends on locomotor behaviour.

Key words: rat, hopping mouse, skeletal muscle, elasticity, *Rattus norvegicus*, *Notomys alexis*.

Introduction

During locomotion, animals expend considerable amounts of metabolic energy on performing mechanical work, which is generated by skeletal muscles. One way to reduce the amount of mechanical work that skeletal muscles have to produce is *via* the storage and re-utilisation of elastic energy in the muscles' series elastic structures (e.g. Biewener *et al.* 1981; Morgan *et al.* 1978). Generally, during the impact (landing) phase of a stride, a proportion of the kinetic and potential energy of the body is converted to and stored as strain energy by stretching the tendons. During take-off, this energy is recovered when the tendons recoil. It is generally believed that this mechanism is advantageous only in larger animals. Small animals have relatively thick tendons, which are strained to a much lower degree during locomotion than is the case in large animals (Biewener *et al.* 1981; Casey, 1992; Pollock and Shadwick, 1994). This applies particularly to kangaroos (Bennett and Taylor, 1995). Biewener and Blickhan (1988) argued that kangaroo rats (*Dipodomys spectabilis*) have hindlimbs that are better designed for acceleration than for elastic energy storage. Perry *et al.* (1988) compared the tension properties of the entire

plantar flexion muscle group in the kangaroo rat *Dipodomys spectabilis* and the rat *Rattus norvegicus*. They concluded that, at their preferred locomotion speeds, muscle stresses were the same for both animals, arguing that the larger-sized muscle group in the kangaroo rats compensated for the loss of front limb support during locomotion.

This study aims to investigate whether the functional design of individual muscle–tendon units in a species is adapted to species size and normal locomotion pattern. In order to address these aims, the elastic and contractile properties of the medial gastrocnemius muscle of two animals, the hopping mouse *Notomys alexis* and the rat *Rattus norvegicus*, are compared. To distinguish differences related to species and size, the data from this study are compared with similar results from previous studies of two differently sized hopping animals, the kangaroo rat *Dipodomys spectabilis* (Biewener and Blickhan, 1988) and the wallaby or pademelon *Thylogale billiardieri* (Morgan *et al.* 1978).

Morphological measurements and elastic properties of tendinous structures of many mammalian species have been

reported previously (e.g. Bennett *et al.* 1986; Pollock and Shadwick, 1994). However, these morphological measurements do not necessarily allow the functional capacity for the utilisation of elastic energy to be accurately predicted: free tendon and aponeurosis may differ in elasticity (Ettema and Huijing, 1993; Zuurbier *et al.* 1994), and muscle fibres contain a significant number of series elastic structures (Morgan, 1977; Ettema and Huijing, 1993). In the present study, the force–stiffness relationship of the series elastic element (SEE) and the length–force curve of the contractile element (CE) of the gastrocnemius muscle were determined. An accurate estimate of the functional capacities for work production and elastic energy storage of the muscle could therefore be obtained. Such a direct comparison of contractile and elastic capacities has not been made previously in relation to locomotor pattern and size. Thus, this study provides additional information to the studies of Biewener *et al.* (1981), Biewener and Blickhan (1988) and Perry *et al.* (1988), who compared different animals regarding this issue.

Materials and methods

Eleven young male rats *Rattus norvegicus* (Berkenhout) (body mass 313 ± 10.7 g, mean \pm S.D.) and four hopping mice *Notomys alexis* (Thomas) (body mass 30.2 ± 2.4 g) were used in this experiment. All animals were bred in captivity. The animals were anaesthetised with pentobarbital (initial dose 10 mg per 100 g body mass, intraperitoneally). In the rat, the medial head of the gastrocnemius (MG) was examined, whereas in the hopping mouse the entire gastrocnemius (G) was used. This was necessary to adjust muscle strength to the specifications of the muscle–puller system that was used. The medial and the lateral head of the rat gastrocnemius do not differ in fibre type and differ only little in fibre length (Woittiez *et al.* 1985). With the aid of morphometric measurements (see below), the data on the hopping mouse gastrocnemius muscle could be compared with MG values. The muscle was freed

from surrounding tissues, leaving its blood supply intact. The sciatic nerve was severed as proximally as possible to leave a long distal nerve end attached to the muscle. The calcaneus was cut to leave a bony attachment at the Achilles tendon, which was then used as an anchoring point to fix the tendon to a metal wire. The wire was connected to the motor of a muscle puller, which was equipped with a strain gauge force transducer (accuracy to within ± 0.05 N) and a linearly variable differential transformer (accuracy to within ± 0.01 mm) in series with the muscle–tendon complex. The femur was scraped clean at the shaft so that it could be clamped and fixed to the muscle–puller fixation table. The position of this table was adjustable relative to the motor to an accuracy of less than 0.02 mm. The muscle was supramaximally activated by electrical stimulation of the severed nerve through a bipolar electrode (100 Hz square-wave pulse train, 0.5 ms, 2 mA). The ambient muscle temperature was maintained at 30 °C, a temperature that allows constant muscle condition under *in situ* situation and is close to the *in vivo* temperature. The muscle–tendon unit was covered with paraffin oil to prevent drying.

Series elastic stiffness of the muscle–tendon unit was measured using 210 Hz small-amplitude (0.2 mm) sinusoidal perturbations lasting 100 ms during the force plateau of a contraction (Fig. 1). The perturbations were applied 400 ms after the onset of activation. Recordings of muscle force and muscle–tendon length were A/D-converted and collected on a computer at a sample frequency of 2500 Hz. Experiments were repeated at different muscle–tendon lengths for two purposes: (i) to change the isometric force level in order to obtain a force–stiffness relationship, and (ii) to obtain a muscle length–force relationship, for which the isometric force level just prior to the length perturbations was used. Optimum length of the muscle–tendon complex (l_0) was defined as the length (in mm) at which maximal isometric force (F_0 , in N) was obtained.

Series elastic stiffness (S , in N mm^{-1}) was defined as the peak-to-peak force difference divided by the peak-to-peak

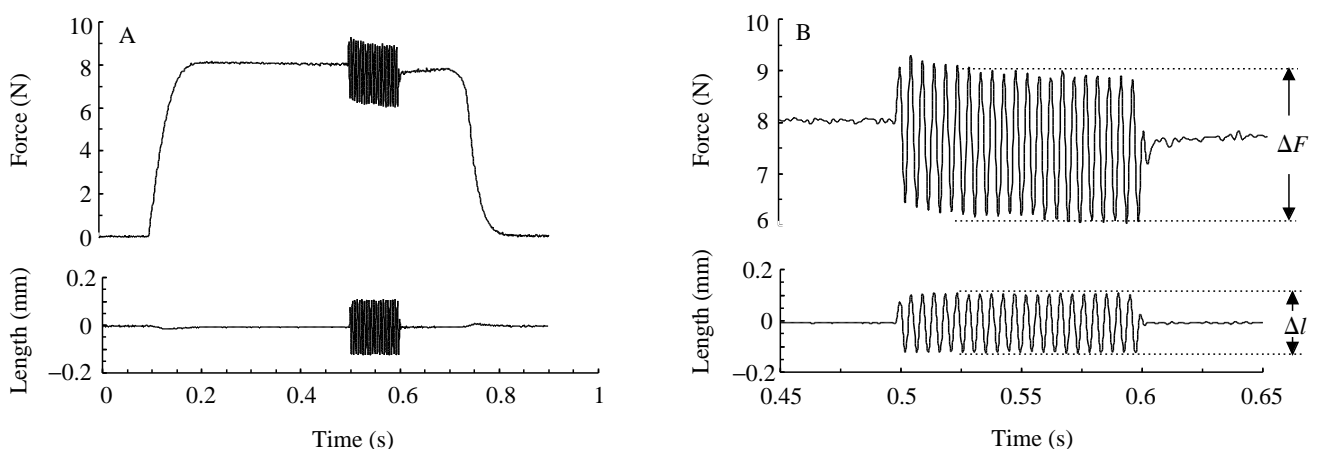


Fig. 1. (A) Force (upper diagram) and length (lower diagram) tracings of a tetanic contraction (hopping mouse gastrocnemius muscle) and 210 Hz sine-wave perturbations. Activation started at 0.1 s and ceased at 0.75 s. (B) Enlargement of A at the time of the sine-wave perturbations. Stiffness was calculated as $\Delta F/\Delta l$, averaged over all sine waves, where l is muscle length and F is force.

length difference during the sine-wave perturbations (Fig. 1) and was corrected for equipment compliance (0.02 mm N^{-1}) (Ettema and Huijing, 1994a). The construction of a force–stiffness curve allowed the calculation of the series elastic force–elongation curve (by integration of compliance, i.e. stiffness⁻¹, over force), and thus the calculation of elastic energy stored in the series elastic element. For this purpose, the force–stiffness data were fitted with a power function ($S=aF^b$). Elastic energy stored at maximal isometric force was used as a functional representation of the capacity for elastic energy storage (CAP_{ee}).

Tendon stress at maximal isometric force could be deduced using the following information. Assuming that tendons in different species have the same Young's modulus (E) of 1.5 GPa (Bennett *et al.* 1986), it was possible to estimate the cross-sectional area for the tendinous tissue from the experimental elastic stiffness values and from the distinction of tendinous stiffness *versus* fibre stiffness (Ettema and Huijing, 1993): the cross-sectional area of the tendons equals $S_{ts} \times l_{ts} / E$, where S_{ts} (in N mm^{-1}) and l_{ts} (in mm) are the stiffness and length of the tendinous structures, respectively. S_{ts} was calculated as $S_{ts} = S \times (S_{ts}/S)$, with the S_{ts}/S value obtained from the literature (Morgan *et al.* 1978; Ettema and Huijing, 1993).

The length–force curve of the muscle–tendon complex was corrected for series elastic elongation to construct the length–force curve of the contractile element (CE) (Ettema and Huijing, 1994b; Ettema, 1995): the length of the contractile element (in mm) was calculated as:

$$\Delta l_{CE} = \Delta l_{MT} - \Delta l_{SEE}, \quad (1)$$

where MT refers to the muscle–tendon complex and Δl refers to the difference between the actual length and the reference length (not to elongation as a function of force). Reference lengths were set at the following values: $\Delta l_{SEE} = 0 \text{ mm}$ at $F = F_0$, $\Delta l_{MT} = 0 \text{ mm}$ at l_0 . Thus, $\Delta l_{CE} = \Delta l_{SEE} = 0 \text{ mm}$ at l_0 and F_0 (F_0 being maximal isometric force). A physical CE optimum length, closely related to fibre length, was calculated as:

$$l_{0-CE} = l_0 - (l_{ts} + \text{elongation}_{SEE \text{ at } F=0}), \quad (2)$$

where ts refers to tendinous structures.

Note that, in equation 2, the calculated elongation of SEE is used rather than Δl_{SEE} . For these calculations (i.e. equations 1 and 2), stiffness measurements were not corrected for the compliance of the muscle puller, since the contractile machinery is connected in series with the series elastic element (SEE) as well as the muscle puller. Thus, the non-corrected compliance represents the compliance 'seen' by the contractile element. Note that CE length changes are a lumped representation of myofibril sliding and associated cross-bridge cycling. SEE behaviour represents all other length changes in the muscle–tendon complex, i.e. tendinous length changes as well as elastic deformation of cross-bridges (Ettema and Huijing, 1993).

Integration of the CE length–force curve from optimum length (l_{0-CE} , i.e. the length at which F_0 is generated) to short

slack length (the shortest length at which active force is generated) provided the contractile work capacity (CAP_{cw}) of the muscle. This work capacity is the theoretical maximum work that the contractile element can generate when shortening from optimum length to slack length at infinitely slow speed. The length–force data were fitted with a second-order polynomial function for the purpose of calculating work capacity. The functional applicability of the contractile work capacity, based on isometric muscle properties, requires information on the muscle's force–velocity properties. Thus, an additional experiment was performed on the muscles of one hopping mouse and five rats. Force–velocity characteristics of the contractile element were determined by applying isokinetic shortening contractions with speeds varying from 5 to 50 mm s^{-1} . A protocol similar to that described by Ettema and Huijing (1988) was used. They showed that isotonic and isokinetic techniques gave similar results as long as the force during isokinetic shortening remained more or less constant. The muscle–tendon complex was brought to a preset length near l_0 at which a tetanic contraction was elicited. The first 50 ms were isometric, after which the muscle was shortened or stretched for 100 ms at a preset velocity. The preset length was chosen such that in the mid-phase of the isokinetic period (after 100 ms of stimulation) optimum length was reached. Force level at l_0 was taken for the determination of the force–velocity relationship. By applying this particular protocol, care was taken that force transients at the moment of force measurement at l_0 were small. Thus, the velocity of the contractile element was very similar to the muscle–tendon velocity. However, muscle–tendon velocity was still corrected for any series elastic length changes according to equation 1 (the correction was always less than 5%).

After termination of the experiments, morphometric measurements were taken. At optimum muscle–tendon length l_0 , the length of tendinous structures (free tendon and aponeurosis) and the length of the most distal fibre bundle (l_{fibre}) were measured to the nearest 0.5 mm. Muscle–tendon length was calculated as fibre length plus the length of the tendinous structures, which is slightly different from the morphological length because of the muscle's pennation angle, but is more closely related to its function. After the length measurements, the muscle was cut at its origin and quickly weighed, both suspended and non-suspended in distilled water to measure mass (to $\pm 1 \text{ mg}$) and volume (V to $\pm 1 \text{ mm}^3$). The muscle's physiological cross-sectional area (PCSA, in mm^2) was calculated as V/l_{fibre} . Furthermore, the 'priority of force' factor (PF) was determined according to Woittiez *et al.* (1986): $\text{PF} = \text{PCSA} \times V^{-2/3}$. Thus, PF is a dimensionless indicator of the relative amount of contractile tissue organised in parallel (enhancing force generation capacity) rather than in series (enhancing shortening capacity).

In the hopping mice, the morphometric measurements were taken for both medial and lateral heads. Thus, with the aid of the medial/lateral ratios of PCSA, fibre length and muscle–tendon length, the force–stiffness and length–force relationships measured on the entire gastrocnemius could be

transformed to relationships for the medial head exclusively. It was assumed that the PCSA ratios of the muscles were a true indication of the ratios of the cross sections of the tendinous structures of the medial and lateral heads.

Results for the hopping mouse and rat were tested for differences based on a two-tailed Student's *t*-test. Force–stiffness and length–force curves were compared by means of an *F*-test for the residual sum of squares, using pooled and separate rat and hopping mouse fits (Crowder and Hand, 1990). Results for the rat were also compared with scaled predicted values from an allometric fit of the hopping mouse, kangaroo rat (Biewener and Blickhan, 1988) and wallaby (Morgan *et al.* 1978) data. A scaling curve for the hopping animals was constructed by a least-squares fit of the muscle–tendon properties (average values for each species) according to $y = k \times M_b^q$, where *y* is the variable in question, *q* is the scaling exponent, *M_b* is body mass (in g) and *k* is a constant. For each individual rat, a prediction of each variable was made on the basis of the scaling curve from the hopping animals. Thus, each rat could be compared with an equally sized hopping equivalent, using a two-tailed Student's *t*-test for paired comparisons. This procedure was only carried out where data for all three hopping animals were available. It should be noted that the purpose of the construction of these scaling curves was to allow a more accurate comparison than a direct comparison of the differently sized hopping mouse and rat would be. As these curves are based on three species, the scaling exponents can only be regarded as a preliminary indication of the allometric comparisons made.

Results

Table 1 shows a selection of morphological and physiological data for the hopping mice and rats, together with similar data for other species obtained from the literature. The data for kangaroo rats (Biewener and Blickhan, 1988) are based on entire gastrocnemius measurements and are corrected for a MG/G mass ratio of 0.4 (A. A. Biewener, personal communication). In the hopping mouse, the MG/G mass ratio was 0.42 ± 0.02 (S.D.) and for the rat 0.49 (Woittiez *et al.* 1985), a value which was supported by a single measurement in this study. Length differences between the medial and lateral head were systematic, but small, and of little influence on the present results.

Hopping mouse versus rat

Elastic properties

Normalised force–stiffness characteristics are shown in Fig. 2A. The differences between the rat and hopping mouse data *versus* the wallaby data (Morgan *et al.* 1978) are striking. However, smaller but significant differences between the hopping mouse and rat data are also present. The hopping mouse shows slightly stiffer normalised SEE properties ($P = 0.02$). It should be noted that series elastic stiffness is a property of a multi-component system (tendon, aponeurosis, fibre elasticity) with different morphological and elastic

properties. This aspect makes normalisation of total stiffness difficult and, thus, results are hard to interpret regarding tissue (tendon, fibre) properties.

Despite the relatively high values of normalised SEE stiffness in the hopping mice, these animals show a higher ratio of elastic energy storage capacity (CAP_{ee}) divided by contractile work capacity. Expressed per gram body mass, CAP_{ee} is also significantly higher for the hopping mouse than for the rat (0.039 *versus* 0.019 mJ g^{-1} , Table 1). Fig. 2B shows the normalised stress–strain curves derived from the data in Fig. 2A. Note that two curves, for one rat and one hopping mouse, show a higher strain than the other curves for both species. This is due to the strong influence of the stiffness measurements at low force levels after numerical integration. The two animals in question showed a slightly lower stiffness at low force levels (approximately 1–5% of F_0) than the other animals. The effect on storage of elastic energy (i.e. the area enclosed by the vertical axis and each stress–strain curve, the area to the left of the curves in Fig. 2B) is negligible. The large slope for the wallaby muscle is a reflection of its low stiffness (see Fig. 2A).

Contractile properties

The length–force properties of the MG of the rat and hopping mouse are presented in Fig. 3. Fig. 3A shows the length–force curves normalised for F_0 and optimum muscle–tendon length (l_{M0}). The ascending limb of the curve, as determined by a linear regression line through the data points on the ascending limb, shows a significant shift to the right for the hopping mouse compared with the rat (*F*-test for residual sum of squares when fitting all pooled data *versus* fitting rat and hopping mouse data separately, $P < 0.01$). This relatively narrow length–force curve is due to the shorter fibres of the hopping mouse (7.3 mm) compared with the length of its tendinous structures (26.7 mm, Table 1). No significant differences were found for the ascending limb of the length–force curves of the contractile element (Fig. 3B). Maximum isometric muscle stress is somewhat higher for the hopping mouse than for the other animals in this study (Table 1). The stress difference between the hopping mouse and rat was statistically significant ($P < 0.05$).

Fig. 4 shows the normalised force–velocity data for five rats (mean \pm S.D.) and one hopping mouse. The data for the rats were averaged for both force and velocity, as the absolute velocities applied in the experiments appeared to result in very similar normalised velocities for all rats. Forces for the hopping mouse were approximately 20% lower than for the rat at the same relative velocity.

Scaling versus interspecies differences

Literature data for other bipedal species (the kangaroo rat *Dipodomys spectabilis* and the wallaby *Thyogale billiardieri*) allow some analysis of scaling effects. On the basis of scaling curves constructed for the three hopping species, a prediction of MG muscle–tendon properties was made for each individual rat (see Table 1). In the hopping animals, MG muscle mass and

Table 1. Morphological and physiological results for the medial gastrocnemius muscle, related to animal size (mass)

Species	N	Mass			Length			Isometric			Stress at F_0			Stiffness at F_0			Capacity for contractile work and elastic energy storage, $CA P_{ee}$		
		Body (g)	Muscle (g)	PCSA (mm ²)	Fibre (mm)	Tendon (mm)	Force priority	Force (N)	Muscle (kPa)	Tendon (MPa)	SEE (N mm ⁻¹)	SEE (mJ)	CE (mJ)	SEE/CE (mJ g ⁻¹)	SEE/body mass (mJ g ⁻¹)	CE plantar flexors (mJ)			
		(S.D.)	(S.D.)	(S.D.)	(S.D.)	(S.D.)	(S.D.)	(S.D.)	(S.D.)	(S.D.)	(S.D.)	(S.D.)	(S.D.)	(S.D.)	(S.D.)	(S.D.)			
<i>Notomys alexis</i>	4	30.2 (2.4)	0.121 (0.016)	15.3 (1.9)	7.3 (0.6)	26.7 (2.6)	0.661 (0.057)	3.6 (0.5)	238 (21)	19 (3)	7.7 (1.7)	1.17 (0.17)	8.07 (1.29)	0.147 (0.036)	0.039 (0.004)	25.9 (4.1)			
<i>Dipodomys spectabilis</i> †	5	103.0	0.542	45.2	9.6	37.6	0.789	9.0	200	22			29.40			97.9			
<i>Rattus norvegicus</i> (S.D.)	11	313.4 (10.7)	0.819 (0.035)	54.1 (4.4)	13.8 (1.2)	30.4 (1.2)	0.659 (0.057)	11.3 (0.9)	209 (22)	24 (N=9)	15.9 (1.2)	6.00 (0.55)	59.62 (5.2)	0.101 (0.007)	0.019 (N=6)	150.8 (13.2)			
<i>Thylogale billiardieri</i> ‡	1	6800.0	13.380	675.0	18.7	130.0	1.245	135.0	200	62	21.1	500	855	0.585	0.074	3591.6			
<i>R. norvegicus</i> versus <i>N. alexis</i>		***	***	***	***	**	—	***	*	**	***	***	***	**	***	***			
Scaling exponent, q		0.85	0.85	0.69	0.17	0.29	0.11	0.66	-0.02	0.23			0.85			0.90			
<i>R. norvegicus</i> versus prediction		***	***	***	***	***	***	***	—	***			*			***			
<i>R. norvegicus</i> :prediction		0.999	0.999	84.4	11.1	52.6	0.878	17.9	211	30			64.89			232.0			

†Data from Biewener and Blickhan (1988); ‡data from Morgan *et al.* (1978). Data for *D. spectabilis* are based on a 0.4 MG/G ratio.

PCSA is physiological cross-sectional area and force priority is defined as $PCSA \times V^{-2.3}$ (Woittiez *et al.* 1986).

Work capacity for plantar flexor group is based on MG work capacity and the relative size of the MG compared with that of other plantar flexors.

Prediction for *R. norvegicus* is based on allometric scaling for hopping animals (*N. alexis*, *D. spectabilis*, *T. billiardieri*) according to: $y = kM_b^q$, where q is the scaling exponent, M_b is body mass, k is a constant and y is the variable in question.

For further explanation of methods and for calculations see text.

*** $P < 0.001$; ** $P < 0.01$; * $P < 0.05$, not significant.

SEE, series elastic element; CE, contractile element; MG, medial gastrocnemius; G, gastrocnemius.

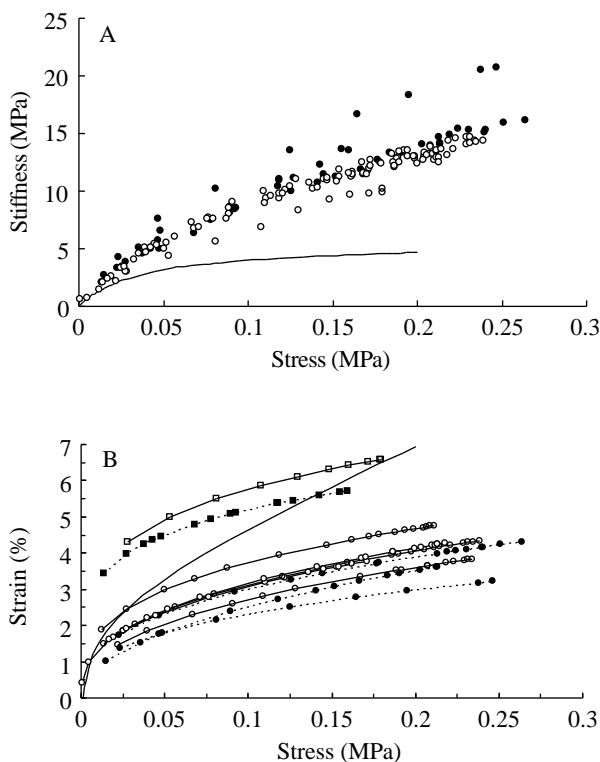


Fig. 2. (A) Normalised stress–stiffness curve for the rat (\circ , $N=6$), the hopping mouse (\bullet , $N=4$) and the wallaby (solid line). Wallaby data are derived from Morgan *et al.* (1978). Data are normalised for muscle–tendon length and physiological cross-sectional area. Note that the stiffness and stress values are based on the cross-sectional area of the muscle, not on the cross section of the tendinous structures. (B) Stress–strain curves based on data in A for the rat (open symbols, solid lines) and hopping mouse (filled symbols, dashed lines). Square symbols indicate two curves with high strain levels (for explanation see text). The solid line without symbols is the curve for the wallaby. Each curve is for a different animal.

contractile work capacity increase less than geometrically (exponent is 0.85, an exponent of 1 indicates geometric scaling) owing to fibre length differences. PCSA and force scale geometrically (exponents are 0.69 and 0.66, respectively, an exponent of 0.67 indicates geometric scaling).

In Table 1, significant differences between the hopping mouse and rat, as well as the rat *versus* its allometric prediction, are shown. The results in Table 1 indicate that the rat deviates significantly from the scaling line for the three hopping species for all variables except muscle stress. The most important differences between the measured values and those predicted from the hopping scaling line for the rat can be summarised as follows: the length of tendinous structures is shorter in the rat than in the hopping species; MG muscle mass and, consequently, contractile work capacity are smaller in the rat than in hopping animals; MG cross-sectional area and isometric force are smaller in the rat; and MG muscle fibres are longer in the rat. In combination, these differences result in a lower force priority for the MG in the rat. That is, given the amount of contractile tissue, the MG muscle has a higher

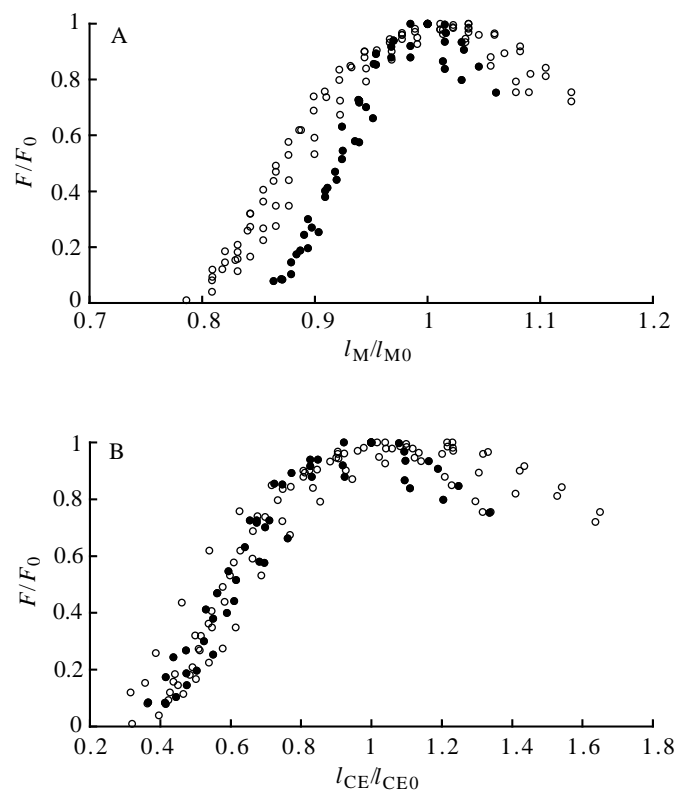


Fig. 3. Length–force data for the rat (\circ , $N=6$) and hopping mouse (\bullet , $N=4$). (A) Data normalised according to optimum muscle–tendon length (l_{M0}). (B) Data normalised according to optimum contractile element (CE) length (l_{CE0}). Note that the CE length is similar to the fibre length corrected for all series elastic elongation, including intrafusal elasticity.

shortening capacity due to long fibres and a lower force-generating capacity due to a small PCSA than in the hopping animals. Contractile work capacity of the entire plantar flexor group is shown in the right-hand column of Table 1. These values are calculated on the basis of MG work capacity and relative muscle sizes. The following values, as a percentage of gastrocnemius mass, were used. The plantaris was regarded to be 17% in the rat (Woittiez *et al.* 1985), 30% in the kangaroo rat (Biewener *et al.* 1981) and approximately 100% in the wallaby (M. B. Bennett, personal communication). For the hopping mouse, the plantaris mass was not determined, but is of significant size and was assumed to be a similar percentage as in the kangaroo rat. The soleus muscle is small (approximately 10% of the gastrocnemius mass) in the wallaby (M. B. Bennett, personal communication) and can be almost ignored in small hopping animals: in the kangaroo rat it is 3% (Biewener *et al.* 1981), in the hopping mouse it is 5% (this study) and in the rat 7% (Woittiez *et al.* 1985). Work capacity for the entire plantar flexor group is about 35% lower in the rat compared with that in the hopping animals.

Deviations of rat elastic energy capacity from the allometric prediction were not tested statistically since the allometric prediction could only be determined from two data points

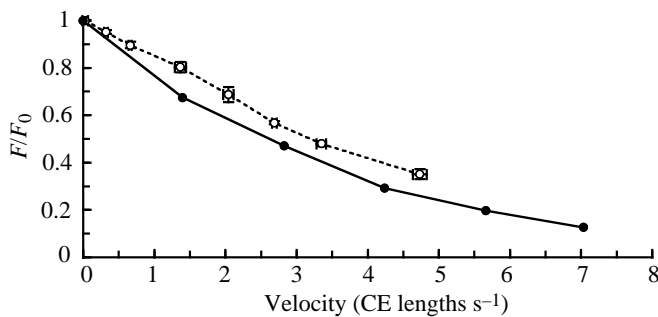


Fig. 4. Normalised force–velocity curves of the contractile element (CE) of the rat (○, dashed line; mean \pm s.d., $N=5$) and one hopping mouse (●, solid line).

(hopping mouse and wallaby). However, both relative elastic capacities are lower in the rat than in the hopping mouse and wallaby.

Tendinous stress at F_0 (Table 1) was estimated as explained in the Materials and methods section for the hopping mouse, rat and wallaby, assuming a Young's modulus of 1.5 GPa for tendon, and using experimental muscle–tendon stiffness values and reported stiffness ratios of the tendinous structures and the entire muscle–tendon complex (1.18 for the wallaby, Morgan *et al.* 1978; 1.42 for the rat, Ettema and Huijing, 1993). For the hopping mouse, the ratio of 1.42 (rat value) was used; a 10% deviation from this ratio did not alter the results significantly. The tendon stress value of 22 MPa for the kangaroo rat was reported by Biewener and Blickhan (1988). It appears that, in hopping animals, tendon stress increases with body mass. The rat MG tendon stress is lower than for its hopping equivalent (scaling exponent=0.23).

Discussion

To compare muscle properties of the rat with those of differently sized hopping species and to distinguish locomotor aspects from scaling aspects, an allometric scaling line was constructed from data for three hopping species. It was assumed that the differences between the three hopping species were purely due to scaling differences. Although this assumption cannot be proved to be correct (data are limited), the data for the three hopping species are in agreement with this assumption. All variables presented in Table 1 demonstrate a logarithmic increase with size. Only the values for the rat, a non-hopping animal, deviate clearly from this pattern.

The rat has relatively long muscle fibres and short tendinous structures, a small muscle mass and PCSA and a low force priority compared with the hopping animals. The functional manifestations of this are low force generation and contractile work capacity, as well as low tendinous stress and relative capacity for storage of series elastic energy for its size.

Normalised contractile properties (CE length–force curve) for the rat do not differ from those for the hopping mouse (Fig. 3B), indicating that no adaptations have occurred in the

contractile mechanism at the microscopic level. However, a 20% higher stress was found in the hopping mouse (Table 1). This difference may be due to a number of reasons, discussed briefly below. (1) The relative amount of parallel connective tissue in the muscle will affect muscle stress. However, if the MG of the hopping mouse contains less connective tissue than that of the rat MG, this would have been indicated by a relatively low passive force for the hopping mouse MG. This was not found in this study (for the hopping mouse, MG passive force was 0.05 N and F_0 was 3.6 N; for the rat, MG passive force was 0.09 N and F_0 was 11.3 N). (2) The variation in fibre length throughout a muscle can also affect muscle stress (Ettema and Huijing, 1994b). However, this phenomenon probably did not cause the stress difference reported here, since it should also have caused a narrower CE length–force curve for the hopping mouse (Ettema and Huijing, 1994b). (3) The muscle stress difference might also be explained by the method used to calculate the cross-sectional area of the muscle. The PCSA calculation was based on measurement of the length of the most distal fibre bundle. The length of the distal fibre bundle may differ from the average fibre length in the MG of the hopping mouse and the rat. More importantly, deviations from the average fibre length may differ between these species, causing different systematic errors in the stress calculations. (4) Another explanation may be found in pennation angles. Pennation angles were not measured in this study, but a smaller pennation angle in the hopping mouse than in the rat could result in increased tension together with reduced normalised velocity, as was found in Fig. 4. With a smaller pennation angle, a larger tension is detected at the tendon for a given fibre tension; at the same time, the contribution to the shortening speed of the muscle by an increasing pennation angle during shortening is reduced (Zuurbier and Huijing, 1992).

Normalised series elastic stiffness

The normalised elastic stiffness of the rat MG is lower than that of the hopping mouse (Fig. 2A). The relatively longer tendons and shorter fibres in the hopping mouse do not necessarily contradict the higher stiffness of its gastrocnemius muscle–tendon complex, because muscle fibre tissue contributes significantly to the series elastic behaviour of muscle–tendon units (Ettema and Huijing, 1993). At F_0 , Ettema and Huijing (1993) found similar normalised stiffness values for tendon and fibre in rat MG and extensor digitorum longus muscles. In this case, the relative lengths of the tendon and fibre have no impact on total stiffness. Note that this does not apply at lower forces, because of the highly compliant 'toe region' of the stress–strain curves of the tendinous structures, which is not apparent in the elastic behaviour of muscle fibres (i.e. cross-bridges and myofilaments). It is feasible that in small animals such as the rat and the hopping mouse, and even in the larger wallaby, tendons are loaded in the toe region of their stress–strain curve for a large proportion of time (e.g. Biewener and Blickhan, 1988; Biewener *et al.* 1981). Such a condition would make the prediction of muscle–tendon stiffness on the basis of tendon/fibre length ratios even more complicated.

Furthermore, ignoring the highly compliant toe region, i.e. using the stiffness of the linear part of the stress–strain curve (Young's modulus) for the calculation of tendon stress, results in an overestimation of tendon stress values for the hopping mouse, rat and wallaby. Lower stress values for these animals than those reported in Table 1 would strengthen the conclusion that tendon stress in the rat is relatively lower than in a similarly sized hopping animal. It should be noted that the normalised stiffness at F_0 also does not fully predict the elastic energy storage capacity. The elastic energy stored is found by integration of the entire force–elongation curve, which is a measure of the complete SEE, not that stored by the tendinous structure only.

Contractile performance

It should be noted that most comparisons made in this study concern the functional design of only one of the plantar flexor muscle–tendon units, rather than the function of the entire plantar flexor system during locomotion. The contractile work capacity of the plantar flexor group was estimated on the basis of muscle mass. The current study indicates that the rat hindlimb muscles have a relatively lower mass, work capacity and force production (MG data only) than those of hopping animals.

It seems likely that adaptation to different locomotion styles is an important factor for muscle mass and work capacity. An important aspect is quadrupedal *versus* bipedal support. Perry *et al.* (1988) showed that kangaroo rats have double the muscular cross-sectional area in the ankle extensors compared with rats. The present results are generally in agreement with their findings.

Taking into account the force–velocity curves shown in Fig. 4, the functional implications of the differences in work capacity found in the present study may only be small. Although the force–velocity characteristics of only one hopping mouse were determined, the small variation between data for different rats indicates that the 20% lower force measurement for the hopping mouse compared with the rat is of significance. Clearly, more information on the dynamic properties of quadrupedal and bipedal animals is needed in order to study possible contractile adaptations to locomotion style.

Utilisation of series elastic energy

Rats and kangaroo rats generate the same muscle stress at their preferred speeds of locomotion (Perry *et al.* 1988). If we assume that this finding also applies to the other species considered in this study, and that the plantar flexor group is evenly used in locomotion, it can be concluded that elastic energy capacity is a valid comparative indicator of the amount of elastic energy that is actually stored in the plantar flexors during unrestricted locomotion. Consequently, the relative capacity values (elastic energy capacity over contractile work capacity, and to some extent elastic energy capacity over body mass) should provide useful information about the utilisation of elastic energy storage in different species. This study

confirms the previous suggestion (e.g. Biewener *et al.* 1981; Pollock and Shadwick, 1994; Bennett and Taylor, 1995) that, with increasing size, hopping animals appear to utilise more elastic energy. The morphological adaptation that guides this principle may be summarised as follows. Larger hopping animals have relatively thin tendons with relatively thick and short muscle fascicles (higher force priority). This increases tendinous stress, without affecting the contractile work capacity, and thus enhances relative elastic energy storage capacity. These results agree with the findings of Biewener and Blickhan (1988) suggesting that small hopping animals are designed more for acceleration by generating high forces than for storage and utilisation of elastic energy: their relatively thick tendons are well designed to transfer impact forces quickly, but limit the storage of elastic energy. High compliance causes loss of peak force due to a long delay in rise in force (Bawa *et al.* 1976).

The situation in the rat is quite different. Apparently, the low muscle forces restrict elastic energy storage to a greater extent than they affect contractile work capacity (because the fibres are relatively long, the work capacity is still high). Thus, normalised for muscle mass, or contractile work capacity, less elastic energy can be stored and reutilised compared with a similarly sized hopping animal.

This study confirms the hypothesis that, in the rat, muscle–tendon systems are not designed to utilise elastic energy to the extent that is found in small hopping animals. This indicates that, although small hoppers seem to rely on elastic energy storage to a lesser extent than their larger counterparts (which is confirmed by the design of their muscle–tendon units), they may still use a significant amount of this series elastic energy. The amount of elastic energy storage at F_0 is approximately 15% of the contractile work capacity for the smallest hopping animal (30 g body mass) of the four species studied. In other words, in an infinitely slow shortening contraction from optimum to short slack length, about 15% of the work done would be of an elastic nature (for the rat this amount is approximately 10%, Table 1). During locomotion, it is likely that this value is much higher because of the high shortening velocities and a smaller amount of shortening than from l_0 to slack length, both reducing contractile work while leaving elastic work almost unaltered. Biewener *et al.* (1981) estimated that, in the locomotion of kangaroo rats, about 14% of the negative work stored in the ankle extensors during a footfall was recovered during take-off. The remainder of the negative work was lost and apparently had to be compensated by contractile work production. Thus, if the gastrocnemius of the hopping mouse is representative of all ankle extensors, the percentage of elastic energy recovery in the hopping mouse may be higher than for the larger kangaroo rat. This is in contradiction to the general trend between elastic energy storage and animal size. It should be noted however, that both animals are small and different techniques were used for the experiments on the hopping mouse (this study) and kangaroo rat (Biewener *et al.* 1981). Clearly, comparisons of other bipedal and quadrupedal species

of small sizes are necessary to substantiate the conclusions drawn here. Preliminary data on movement patterns of the gastrocnemius during hopping and running indicate that, during hopping, large eccentric contractions occur at the onset of contraction in hopping animals (G. J. C. Ettema, unpublished data; Biewener and Blickhan, 1988) which are absent in a the running rat (G. J. C. Ettema, unpublished data). Such eccentric contractions enhance the storage of elastic energy because of high peak forces (Biewener and Blickhan, 1988; Ettema *et al.* 1990). These findings are in agreement with the series elastic differences between the MG of the rat and of hopping animals.

The author wishes to acknowledge M. B. Bennett for constructive comments on the first draft of this manuscript and for providing unpublished data on the pademelon.

References

- BAWA, P., MANNARD, A. AND STEIN, R. B. (1976). Effects of elastic loads on the contractions of cat muscles. *Biol. Cybernetics* **22**, 129–137.
- BENNETT, M. B., KER, R. F. AND DIMERY, N. J. (1986). Mechanical properties of various mammalian tendons. *J. Zool., Lond.* **209**, 537–548.
- BENNETT, M. B. AND TAYLOR, G. C. (1995). Scaling of elastic strain energy in kangaroos and the benefits of being big. *Nature* **378**, 56–59.
- BIEWENER, A., ALEXANDER, R. McN. AND HEGLUND, N. C. (1981). Elastic energy storage in the hopping of kangaroo rats (*Dipodomys spectabilis*). *J. Zool., Lond.* **195**, 369–383.
- BIEWENER, A. A. AND BLICKHAN, R. (1988). Kangaroo rat locomotion: design for elastic energy storage or acceleration? *J. exp. Biol.* **140**, 243–255.
- CASEY, T. M. (1992). Energetics of locomotion. In *Advances in Comparative and Environmental Physiology Mechanics of Animal Locomotion*, vol. 11 (ed. R. McN. Alexander), pp. 251–275. Berlin: Springer-Verlag.
- CROWDER, M. J. AND HAND, D. J. (1990). *Analysis of Repeated Measures*. London: Chapman & Hall.
- ETTEMA, G. J. C. (1995). Contractile behaviour in skeletal muscle–tendon unit during small amplitude sine wave perturbations. *J. Biomech.* (in press).
- ETTEMA, G. J. C. AND HUIJING, P. A. (1988). Isokinetic and isotonic force–velocity characteristics of rat EDL at muscle optimum length. In *Biomechanics XI-A, International Series on Biomechanics 7-A* (ed. G. de Groot, A. P. Hollander, P. A. Huijing and G. J. van Ingen Schenau), pp. 58–62. Amsterdam: Free University Press.
- ETTEMA, G. J. C. AND HUIJING, P. A. (1993). Series elastic properties of rat skeletal muscle: distinction of series elastic components and some implications. *Neth. J. Zool.* **43**, 306–325.
- ETTEMA, G. J. C. AND HUIJING, P. A. (1994a). Frequency response of rat gastrocnemius medialis in small amplitude vibrations. *J. Biomech.* **27**, 1015–1022.
- ETTEMA, G. J. C. AND HUIJING, P. A. (1994b). Effects of distribution of muscle fiber length on active length–force characteristics of rat gastrocnemius medialis. *Anat. Rec.* **239**, 414–420.
- ETTEMA, G. J. C., HUIJING, P. A., VAN INGEN SCHENAU, G. J. AND DE HAAN, A. (1990). Effects of prestretch at the onset of stimulation on mechanical work output of rat medial gastrocnemius muscle–tendon complex. *J. exp. Biol.* **152**, 333–351.
- MORGAN, D. L. (1977). Separation of active and passive components of short-range stiffness of muscle. *Am. J. Physiol.* **232**, C45–C49.
- MORGAN, D. L., PROSKE, U. AND WARREN, D. (1978). Measurements of muscle stiffness and the mechanism of elastic storage of energy in hopping kangaroos. *J. Physiol., Lond.* **282**, 253–261.
- PERRY, A. K., BLICKHAN, R., BIEWENER, A. A., HEGLUND, N. C. AND TAYLOR, C. R. (1988). Preferred speeds in terrestrial vertebrates: are they equivalent? *J. exp. Biol.* **137**, 207–219.
- POLLOCK, C. M. AND SHADWICK, R. E. (1994). Relationship between body mass and biomechanical properties of limb tendons in adult mammals. *Am. J. Physiol.* **266**, R1022–R1031.
- WOITTEZ, R. D., BAAN, G. C., HUIJING, P. A. AND ROZENDAL, R. H. (1985). Functional characteristics of the calf muscles of the rat. *J. Morph.* **184**, 375–387.
- WOITTEZ, R. D., HEERKENS, Y. F., HUIJING, P. A., RIINSBURGER, W. H. AND ROZENDAL, R. H. (1986). Functional morphology of the m. gastrocnemius medialis of the rat during growth. *J. Morph.* **187**, 247–258.
- ZUURBIER, C. J., EVERARD, A. J., VAN DER WEES, P. AND HUIJING, P. A. (1994). Length–force characteristics of the aponeurosis in the passive and active muscle condition and in the isolated condition. *J. Biomech.* **27**, 445–453.
- ZUURBIER, C. J. AND HUIJING, P. A. (1992). Influence of muscle geometry on shortening speed of fibre, aponeurosis and muscle. *J. Biomech.* **25**, 1017–1026.